

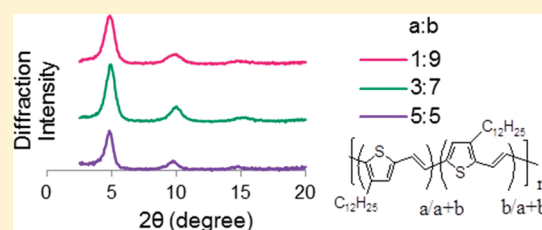
## Poly(3-dodecylthienylenevinylene)s: Regioregularity and Crystallinity

Cheng Zhang,<sup>\*,†,‡</sup> Jianyuan Sun,<sup>†</sup> Rui Li,<sup>†</sup> Sam-Shajing Sun,<sup>‡,\*</sup> Evan Lafalce,<sup>§</sup> and Xiaomei Jiang<sup>§</sup><sup>†</sup>Department of Chemistry and Biochemistry, South Dakota State University, Brookings, South Dakota 57007, United States<sup>‡</sup>Center for Materials Research, Norfolk State University, Norfolk, Virginia 23504, United States<sup>§</sup>Department of Physics, University of South Florida, 4202 E Fowler Ave, Tampa, Florida 33620, United States

Supporting Information

**ABSTRACT:** A series of poly(dodecylthienylenevinylene)s, C<sub>12</sub>-PTVs-*a*:*b*, with tunable regioregularity and solubility have been synthesized using two isomeric comonomers with molar ratios from 0:10 to 5:5, and characterized by NMR spectroscopy, differential scanning calorimetry, absorption spectroscopy, cyclovoltammetry, and X-ray diffraction. For the first time, the aromatic and olefinic <sup>1</sup>H NMR peaks of regioregular head–tail C<sub>n</sub>-PTVs are clearly assigned. No major difference in XRD peak intensity is observed among regiorandom and fully regioregular C<sub>12</sub>-PTVs.

V<sub>oc</sub> of C<sub>12</sub>-PTVs-*a*:*b* and PC<sub>60</sub>BM blend solar cells are in the range of 0.43 to 0.51 V and consistently decrease as regioregularity is reduced. C<sub>12</sub>-PTV-3:7:PC<sub>60</sub>BM solar cells give the highest short-circuit current and practically same efficiency as that of C<sub>12</sub>-PTV-1:9:PC<sub>60</sub>BM devices. The results suggest a new strategy to enhance processability of optoelectronic polymers without sacrificing their crystallinity and device performance.



## 1. INTRODUCTION

Semiconducting polymers have been intensively studied for photovoltaic applications.<sup>1–3</sup> Their optoelectronic properties are highly dependent on regioregularity of side chains and chain organization in the solid state.<sup>4,5</sup> For example, vibronic features in the UV–vis absorption and XRD peaks were observed for 98.5% regioregular (RR) P3HT films, but not for regiorandom P3HT.<sup>6</sup> Highly regioregular poly(3-alkylthiophene)s tend to have lower optical band gap,<sup>6</sup> higher hole mobility<sup>7,8</sup> and are widely used in solar cell devices.<sup>9–12</sup> Better performance has also been reported for fully regioregular poly[(2-methoxy-5-(3',7'-dimethyloctyloxy))-1,4-phenylenevinylene] (MDMO-PPV).<sup>13</sup>

Poly(thienylenevinylene)s (PTVs) have been intensively studied for photovoltaic applications,<sup>14–31</sup> due to their relatively low bandgaps (1.65 eV),<sup>25</sup> and good transport properties ( $\mu_h = 1.5 \times 10^{-3} \text{ cm}^2/(\text{Vs})$ ).<sup>15,19,21,26–30</sup> Solar cell efficiencies of 0.8–0.92% have been reported for monosubstituted C<sub>6</sub>-PTVs.<sup>21</sup> With poly[3-(hexyloxy)thienylenevinylene] synthesized by the Stille coupling reaction, a power conversion efficiency of 2.01% has been obtained.<sup>31</sup> Recently, we reported the first synthesis of a fully regioregular monosubstituted C<sub>12</sub>-PTV polymer using the Horner–Emmons reaction.<sup>32</sup> However, it was found practically insoluble in common organic solvents such as chloroform and chlorobenzene at room temperature. Solubility is also poor for fully regioregular MDMO-PPV,<sup>33</sup> but can be improved by copolymerizing two isomeric comonomers.<sup>34</sup> In this work, two isomeric comonomers, each carrying a phosphonate and an aldehyde group, are synthesized and copolymerized using the Horner–Emmons reaction to produce a series of C<sub>12</sub>-PTVs-*a*:*b* with molar feed ratios ranging from 0:10 to 5:5. The series of C<sub>12</sub>-PTVs-*a*:*b* synthesized provide an opportunity to

examine the influence of regioregularity on crystallinity of the polymer in the solid state. The analyses of the polymers by NMR, DSC, and XRD reveal an unusual correlation between regioregularity and crystallinity of C<sub>12</sub>-PTVs. The results of solar cells fabricated from C<sub>12</sub>-PTVs-*a*:*b* and PC<sub>60</sub>BM blends indicate that the photovoltaic performance of these polymers does not have a strong dependence on their regioregularity. The new finding suggests that regiorandomness may be introduced into certain classes of conjugated polymers to improve the processability without sacrificing optoelectronic performance.

## 2. EXPERIMENTAL SECTION

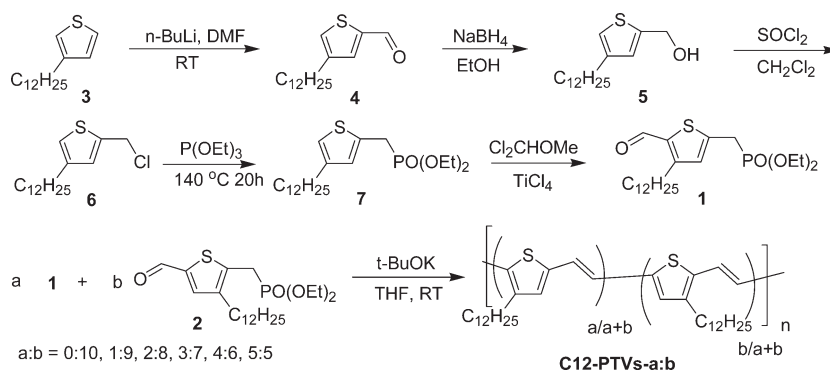
**Starting Materials and Instrumentation.** All starting materials, reagents, and solvents were purchased from commercial sources (Sigma Aldrich and Fisher-Scientific) and used as received. NMR spectra were obtained from a Bruker Advance 300 MHz spectrometer with TMS as the internal reference. UV–vis absorption data were collected on a Perkin-Elmer Lambda 900 Spectrophotometer. Differential scanning calorimetry (DSC) data were collected on a Perkin-Elmer DSC-6. Measurements of polymer molecular weights were done on a Viscotek GPC system with a UV–vis absorption detector at the ambient temperature using tetrahydrofuran as the solvent. Polystyrene standards were used for conventional calibration.

**Cyclovoltammetry.** Electrochemical studies were performed on a Bioanalytical (BAS) Epsilon-100w trielectrode cell system. Three electrodes are a Pt working electrode, an ancillary Pt electrode, and a silver reference electrode in a CH<sub>3</sub>CN solution of 0.01 M AgNO<sub>3</sub> and 0.1 M

Received: February 23, 2011

Revised: July 15, 2011

Published: July 25, 2011

Scheme 1. Synthesis of C<sub>12</sub>-PTVs-*a:b* with Different Regioregularity

tetrabutylammonium hexafluorophosphate, TBA-HFP. The polymer samples were dissolved in hot *o*-dichlorobenzene and then dip coated onto the Pt working electrode. The measurements were performed in a N<sub>2</sub>-purged 0.1 M TBA-HFP/acetonitrile solution at a scan rate of 100 mV/s. Between the experiments, the surface of the electrodes were cleaned or polished. Ferrocene (2 mM in 0.10 M TBA-HFP/CH<sub>3</sub>CN solution) was used as an internal reference standard and its HOMO level of −4.80 eV was used in calculations.

**2-Hydroxymethyl-4-dodecylthiophene (5).** This compound was obtained by reduction of 4-dodecylthiophene-2-carboxaldehyde (**4**, 22.1 mmol, 6.20 g) in a manner similar to that used for its isomer.<sup>32</sup> Yield: 5.90 g, 95.8%. <sup>1</sup>H NMR (CDCl<sub>3</sub>): δ 0.88 (t, 3H, *J* = 7.0 Hz), 1.2–1.4 (m, 18H), 1.58 (m, 2H), 1.98 (s, broad, 1H, OH), 2.55 (t, 2H, *J* = 7.9 Hz), 4.75 (s, 2H), 6.84 (s, 2H, two proton peaks complete overlapped). <sup>13</sup>C NMR (CDCl<sub>3</sub>): δ 14.15, 22.72, 29.40 (two carbon peaks overlapped), 29.52, 29.65, 29.69, 29.72 (three carbon peaks overlapped), 30.48, 31.96, 59.96, 119.92, 126.85, 143.10, 143.69. The crude product was pure enough to be used in the next step. A fraction of the crude product was purified for elemental analysis by silica gel column chromatography using ethyl acetate/hexanes (1:15, v:v) as the eluent. Anal. Calcd: C, 72.28; H, 10.7. Found: C, 72.00; H, 10.60.

**2-Chloromethyl-4-dodecylthiophene (6).** This was prepared from compound **5** (20.9 mmol, 5.90 g) in a manner similar to that used for its isomer.<sup>32</sup> Yield of the crude product: 5.02 g, 79.5%. <sup>1</sup>H NMR (CDCl<sub>3</sub>): δ 0.88 (t, 3H, *J* = 7.0 Hz), 1.2–1.4 (m, 18H), 1.58 (m, 2H), 1.98 (s, broad, 1H, OH), 2.54 (t, 2H, *J* = 7.9 Hz), 4.76 (s, 2H, CH<sub>2</sub>Cl), 6.89 (s, 1H), 6.91 (s, 1H). <sup>13</sup>C NMR (CDCl<sub>3</sub>): δ 14.15, 22.72, 29.33, 29.40, 29.48, 29.62, 29.69 (2C), 19.71, 30.37, 30.41, 31.95, 40.69, 121.38, 129.02, 139.67, 143.17. The crude product was pure enough to pass elemental analysis. Anal. Calcd: C 67.85, H 9.71. Found: C 67.93, H 9.65.

**(4-Dodecylthiophen-2-ylmethyl)phosphonic Acid Diethyl Ester (7).** This was prepared from compound **6** (16.6 mmol, 5.02 g) and purified in a manner similar to that used for its isomer,<sup>32</sup> except that 20 h was needed instead of 4.5 h at 140 °C. Yield: 5.8 g, 87%. <sup>1</sup>H NMR (CDCl<sub>3</sub>): δ 0.88 (t, 3H, *J* = 7.0 Hz), 1.12–1.45 (m, 24H), 1.58 (m, 2H), 2.54 (t, 2H, *J* = 7.9 Hz), 3.31 (t, 2H, *J* = 20.7 Hz, −CH<sub>2</sub>P), 4.07 (m, 4H, P−O−CH<sub>2</sub>−), 6.74 (s, 1H), 6.82 (d, 1H, *J* = 3.0 Hz). <sup>13</sup>C NMR (CDCl<sub>3</sub>): δ 14.13, 16.39 (d, OCH<sub>2</sub>CH<sub>3</sub>, *J* = 6.0 Hz), 22.70, 28.20 (d at 27.25 and 29.14, *J* = 143.2 Hz, PCH<sub>2</sub>Th), 29.31, 29.37, 29.49, 29.62, 29.65, 29.68 (two carbons), 30.40, 30.48, 31.93 (ThCH<sub>2</sub>), 62.39 (d, *J* = 6.6 Hz), 119.16 128.79 (d, *J* = 8.2 Hz, coupled with P), 131.99 (d, *J* = 10 Hz), 143.34. Anal. Calcd: C, 62.65; H, 9.76; S, 7.97. Found: C, 62.51; H, 9.75; S, 7.92.

**4-Dodecyl-5-formyl-thiophen-2-ylmethyl)phosphonic Acid Diethyl Ester (1).** This was prepared from **7** (5.80 g, 14.4 mmol) and purified in a manner similar to that used for its isomer.<sup>32</sup> The yield was nearly quantitative. <sup>1</sup>H NMR (CDCl<sub>3</sub>): δ 0.88 (t, 3H, *J* = 7.0 Hz),

1.15–1.45 (m, 24H), 1.65 (m, 2H), 2.90 (t, 2H, *J* = 8.1 Hz), 3.35 (d, 2H, *J* = 21.7 Hz, −CH<sub>2</sub>P), 4.10 (m, 4H, P−O−CH<sub>2</sub>−), 6.93 (d, 1H, *J* = 3.0 Hz, coupled with P), 9.96 (s, 1H, CHO). <sup>13</sup>C NMR (CDCl<sub>3</sub>): δ 14.13, 16.40 (d, *J* = 5.5 Hz, OCH<sub>2</sub>CH<sub>3</sub>), 22.69, 28.49, 29.02 (d, *J* = 142.7 Hz, PCH<sub>2</sub>), 29.30, 29.35, 29.38, 29.53, 29.62 (two carbons), 29.65, 31.37, 31.91, 62.68 (d, *J* = 6.6 Hz, OCH<sub>2</sub>CH<sub>3</sub>), 131.26 (d, *J* = 8 Hz), 137.02 (d, *J* = 3.3 Hz), 143.13 (d, *J* = 9.9 Hz), 153.35 (d, *J* = 3.8 Hz), 181.72. Anal. Calcd: C, 61.37; H, 9.13. Found: C, 61.36; H, 9.06.

**C<sub>12</sub>-PTVs-*a:b*.** In a glovebox, a solution of *t*-BuOK (1.2 eq, 88.6 mg) in THF (3 mL) was added over 3 min to a solution of **1** and **2** (263 mg, 0.611 mmol in a molar ratio of *a:b*) in THF (3 mL) at the room temperature. The solution became blue immediately after addition of the base. Thirty minutes after the addition, the reaction mixture was dropped into vigorously stirred methanol (40 mL). The polymer product was collected by filtration and washed with methanol until the filtrate became colorless. Typical yield: 93%. <sup>1</sup>H NMR (CDCl<sub>3</sub>) peaks are similar for all polymer products with different comonomer feed ratios: δ 0.88 (t, 3H), 1.2–1.4 (m, 18H), 1.62 (m, 2H), 2.62 (t, 2H), 6.77 (s, 1H), 6.89 (d, 1H, *J* = 15.8 Hz), 7.00 (d, 1H, *J* = 15.8 Hz).

### 3. RESULTS AND DISCUSSION

**Synthesis of Polymers and Model Compounds.** C<sub>12</sub>-PTVs-*a:b* are synthesized via the Horner–Emmons reaction between the aldehyde and phosphonate groups of difunctionalized comonomers **1** and **2** (Scheme 1). **2** was synthesized according to previously established procedure.<sup>32</sup> **1** was synthesized in four steps from **4**, which was obtained from formylation of 3-dodecylthiophene by *n*-BuLi and DMF with a selectivity of 87% or by POCl<sub>3</sub> and DMF with a selectivity of 24%. **4** was separated from **9** (structure shown in Scheme 2) by silica gel column chromatography using low polarity eluent (EtOAc/hexanes = 1/50 by volume). From **4** on, the scheme and synthetic procedures are similar to that used for the synthesis of **2**. The crude product **1** was carefully purified using a silica gel column to ensure high purity. The overall yield of the synthesis of **1** from **3** was as high as 57%.

Relative reactivities of **1** and **2** were tested by treating a THF solution of the two comonomers in 1:1 ratio with 0.67 equivalent of *t*-BuOK, followed by <sup>1</sup>H NMR analysis of the test reaction mixture. The ratio of unreacted **1** and **2** was found to be 1:0.73, indicating that the two monomers have similar Horner–Emmons reactivity. Polymerization of a mixture of **1** and **2** was performed in a glovebox with different feed ratios (0:10, 1:9, 2:8, 3:7, 4:6, and 5:5). The reactions were instantaneous as evident from immediate color change and viscosity increase upon addition of

## Scheme 2. Synthesis of Model Compounds

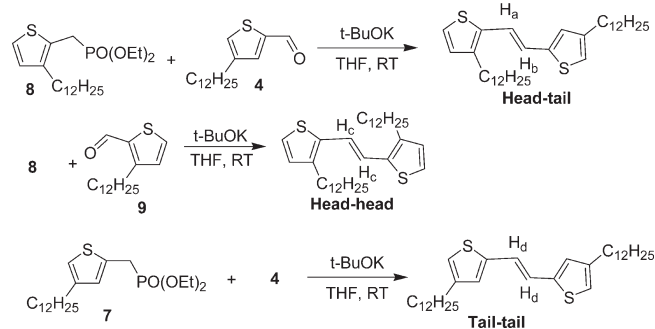


**Table 1.** Molecular Weights of  $C_{12}$ -PTVs-*a:b* in  $\text{kg} \cdot \text{mol}^{-1}$  Measured by GPC with Polystyrenes as the Calibration Standards

| <i>a:b</i> | $M_w$ | $M_n$ | $M_p$ | PDI  |
|------------|-------|-------|-------|------|
| 0:10       | 20.9K | 7.2K  | 12.8K | 2.9  |
| 1:9        | 26.0K | 8.3K  | 24.0K | 3.14 |
| 2:8        | 30.8K | 10.1K | 24.7K | 3.04 |
| 3:7        | 43.8K | 11.8K | 35.7K | 3.71 |
| 4:6        | 59.6K | 13.2K | 43.8K | 4.5  |
| 5:5        | 60.0K | 12.3K | 33.6K | 4.86 |

$t\text{-BuOK}$ .  $C_{12}$ -PTV-1:9 and -2:8 were still poorly soluble in the reaction solvent (THF) and precipitated out of the reaction solution during the polymerization, similar to the case of 0:10.<sup>32</sup> As the ratio approached 5:5, solubility of the polymer products became better. No precipitation was observed for 4:6 and 5:5. Consequently, the polymer weight average molecular weight ( $M_w$ ) increased consistently from 19 to 60 K as the feed ratio changed from 1:9 to 5:5 (Table 1).

Three model compounds, head–tail, head–head and tail–tail, were also synthesized according to Scheme 2 from compounds 4, 7, 8, and 9.<sup>32</sup> Proton NMR spectra of these compounds and all  $C_{12}$ -PTVs-*a:b* are shown in Figure 1. The olefinic protons in the model compounds are labeled (Scheme 1). The two protons ( $H_a$  and  $H_b$ ) in the head–tail compound give two doublets (6.91/6.96 ppm and 6.99/7.06 ppm with a common coupling constant of 15.7 Hz. In the  $^1\text{H}$  NMR spectrum of  $C_{12}$ -PTVs-0:10, the two doublets shifted slightly to 6.86/6.91 ppm and 6.98/7.03 ppm.  $C_{12}$ -PTV-0:10 is 100% regioregular by the nature of the monomer (2) and the polymerization reaction.<sup>33</sup> Weak peaks at 6.84, 7.00, 7.06, and 7.09 ppm in  $C_{12}$ -PTV-0:10 spectrum are presumably due to terminal units since the number average  $M_n$  is only 7.2  $\text{kg} \cdot \text{mol}^{-1}$  (corresponding to a nominal degree of polymerization of 26). As the ratio changes from 0:10 to 5:5, the following were observed: (1) the weak peaks further diminishes as molecular weight of polymer increases, and (2) the major peaks at 6.91 and 6.98 ppm became relatively stronger at the expense of the minor peaks at 6.86 and 7.03 ppm. The weakening of the minor peaks is due to the decrease of the content of H–T units and the growth of the two major peaks is due to overlapping of the olefinic protons of H–H and T–T units, both of which produce a singlet peak as in the two corresponding model compounds. Since the  $H_c$  peak of the H–H model compound appears at the lower field (higher

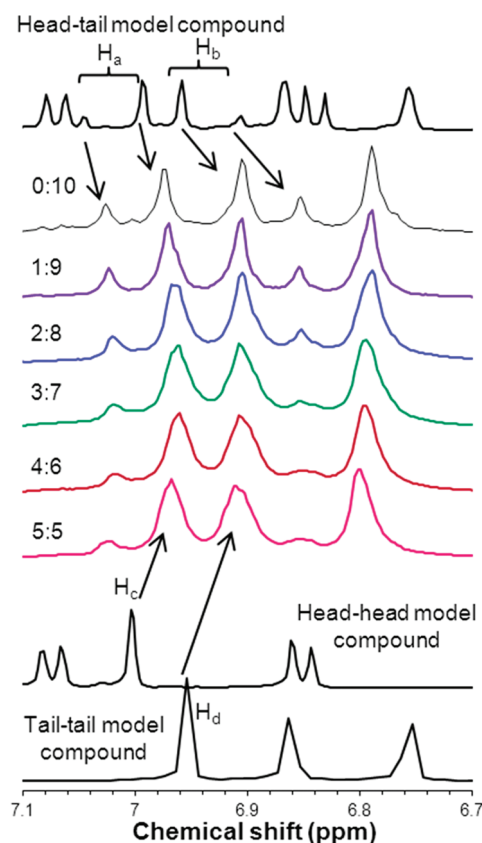


**Figure 1.** Aromatic region of the  $^1\text{H}$  NMR spectra of  $C_{12}$ -PTVs-*a:b* in  $\text{CDCl}_3$ .

chemical shift), the major polymer peak at 6.98 ppm is assigned to the olefinic proton in the H–H unit (together with the olefinic proton in the H–T unit that is next to the H thiophene) and the one at 6.91 ppm is assigned to the olefinic protons in T–T units (together with the other olefinic proton in the H–T unit). The assignment of H–H and T–T olefinic protons is in agreement with the spectrum of 100% H–H/T–T polymer in the literature.<sup>25</sup> Tail–head (T–H) units were also produced when the two isomeric monomers were copolymerized; however, spectroscopically they are not distinguishable from the H–T units. From the changes in relative peak intensities of the major and minor peaks, the combined content of H–T and T–H can be estimated. As the peaks at 6.98 and 7.03 ppm are less broadened than those at 6.86 and 6.91 ppm, their peak heights are measured (with consideration of partial overlap between neighboring peaks) and the ratios, given in Table 2. The contents of H–T and T–H vinylene units ( $f_{\text{HT,TH}}$ ) in nonfully regioregular  $C_{12}$ -PTVs can be estimated using the following equation, which is based on the understanding that the intensity lost at 7.03 ppm,  $(1 - f_{\text{HT,TH}})$ , is gained at 6.98 ppm.

$$\frac{\text{relative intensity at 6.98 ppm}}{\text{relative intensity at 7.03 ppm}} = \frac{2.38 + (1 - f_{\text{HT,TH}})}{1 + f_{\text{TH,HT}}} = \text{measured peak ratio}$$

With this equation the contents of H–T and T–H are estimated from the measured peak ratios in Table 2. The contents of H–T and T–H (Table 2) in both 4:6 and 5:5 polymers are close to the expected value (50%) of a fully regiorandom  $C_{12}$ -PTV.



The analysis performed here can be used to re-examine the chemical structures of previously reported monoalkylated PTVs. For example, the  $^1\text{H}$  NMR spectrum of chloroform-extract fraction of the Stille  $\text{C}_{12}$ -PTV<sup>25</sup> looks quite similar to those of  $\text{C}_{12}$ -PTVs-*a:b*; however, the corresponding peak ratio is about 9.8, even higher than the ratio for  $\text{C}_{12}$ -PTV-5:5 (a fully regiorandom polymer), suggesting that the Stille  $\text{C}_{12}$ -PTV is regiorandom and also contains significant amount of defects that add to the NMR intensity in the region of the major olefinic proton peaks.

The  $^{13}\text{C}$  NMR spectra of 0:10 and 5:5 polymers are shown in Figure 2. Introduction of regiorandomness appears to have little effect on the chemical shifts of  $\text{sp}^3$  carbons in the side chains, but cause each of the aromatic and olefinic carbon peaks to split into multiple peaks.

**Thermal and Optical Characterization.** It was observed, as expected, that the tendency of  $\text{C}_{12}$ -PTVs-*a:b* to crystallize from solutions decreases as the molar ratio changes from 0:10 to 5:5.<sup>33</sup> This is in good agreement with the results of differential scanning calorimetric measurements of  $\text{C}_{12}$ -PTVs-*a:b* (Figure 3) in which every polymer shows two endothermic peaks in the ranges of 127–205 °C and 190–269 °C. Both the peak temperatures and enthalpy changes of the first peak (Table 2) decrease as regiorandomness decreases. In the literature, lower melting temperatures (e.g., < 50 °C for P3DDT) have been reported for regiorandom P3ATs<sup>35</sup> as compared to those of regioregular P3ATs (e.g., ~156 °C for P3DDT<sup>36</sup>). However, in regiorandom P3ATs, the melting peaks were assigned the melting of the side chain domains and crystallinity due to main chain packing was not reported. In RR P3ATs, melting peaks are most likely due to transitions from crystalline state to nematic mesophase and

mesophase to isotropic liquid.<sup>36</sup> Since regiorandom  $\text{C}_{12}$ -PTVs have similar crystallinity as highly regioregular ones (see the XRD section), their thermal behaviors are not fundamentally different from regioregular ones. XRD measurements of selected samples heated at different temperatures will provide more information about the nature of the two transitions.

The UV–vis absorption spectra of  $\text{C}_{12}$ -PTVs-*a:b* are shown in Figure 4. They all have the vibronic features similar to that observed for fully regioregular  $\text{C}_{12}$ -PTV.<sup>32</sup> This is in contrast to poly(3-hexylthiophene) which show vibronic features only when the polymer is highly regioregular.<sup>6,37</sup>  $\text{C}_{12}$ -PTVs-1:9 and -2:8 are not fully dissolved at the concentration of 0.1 mM (based on the repeat unit) at room temperature as indicated by the aggregate (shoulder) peaks, which was also observed for fully regioregular  $\text{C}_{12}$ -PTV.<sup>32</sup> When the chloroform solutions of  $\text{C}_{12}$ -PTVs-1:9 and -2:8 were boiled immediately before the absorption scan, the shoulder peak disappeared, along with a small blue shift in peak absorption wavelength. In the hot solutions, the vibronic peak of higher energy became stronger than the lower energy peak. Similar temperature dependence of the absorption peaks has been reported for poly(2,5-bis(2'-ethylhexyl)-1,4-phenylenevinylene), and was attributed to the changes in the electron–phonon couplings due to the interaction with different phonon modes at different temperature ranges.<sup>38</sup> The absorption

**Table 2.** Intensity (Height) Ratio of Peaks at 6.98 at 7.03 ppm, and calculated combined percentages of H-T and T-H in  $\text{C}_{12}$ -PTVs

| monomer ratio ( <i>a:b</i> ) | peak height ratio | % HT + TH (calculated) | transition peak $T_s$ (°C) | $\Delta H$ of 1st transition (J/g) |
|------------------------------|-------------------|------------------------|----------------------------|------------------------------------|
| 0:10                         | 2.38              | --                     | 205/~269                   | 21.1                               |
| 1:9                          | 2.69              | 91.6                   | 160/233                    | 17.7                               |
| 2:8                          | 3.54              | 74.4                   | 146/229                    | 15.4                               |
| 3:7                          | 4.99              | 56.4                   | 136/199                    | 15.2                               |
| 4:6                          | 5.62              | 51.1                   | 127/193                    | 15.0                               |
| 5:5                          | 5.89              | 49.0                   | 127/190                    | 13.1                               |

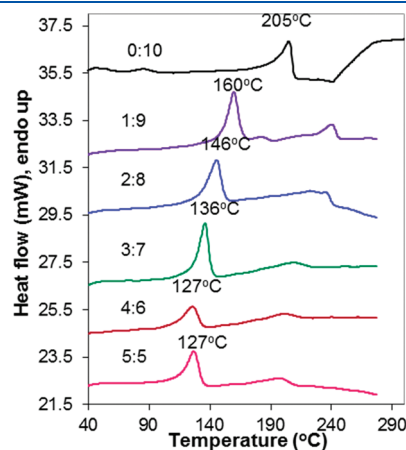


**Figure 3.** DSC scans of  $\text{C}_{12}$ -PTVs-*a:b* in nitrogen at 10 °C/min. Sample weight: 10 mg. All samples were preheated to 230 at 10 °C/min, then cooled at a rate of 5 °C/min to RT. Shown here are the results of the second heating of the preheated samples.

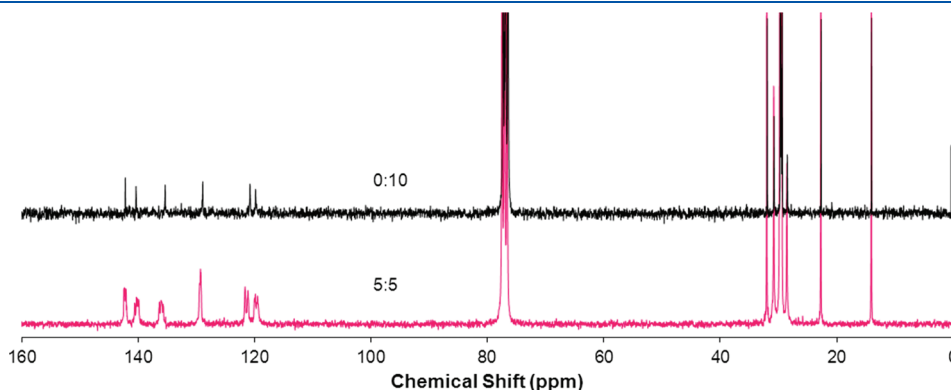


**Figure 2.**  $^{13}\text{C}$  NMR spectra of  $\text{C}_{12}$ -PTVs-*a:b* in  $\text{CDCl}_3$ .

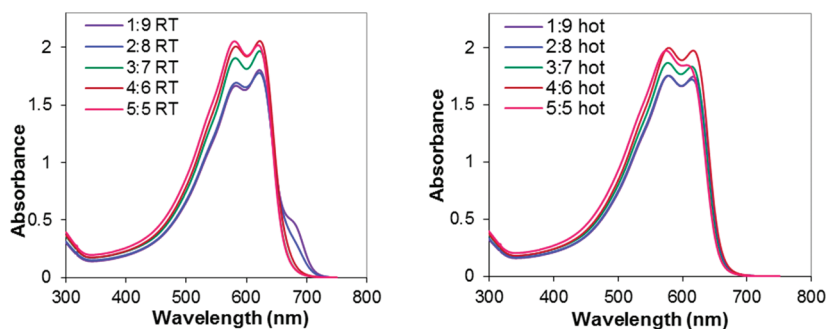


**Figure 4.** UV-vis absorption spectra of 0.1 mM chloroform solutions of  $C_{12}$ -PTVs-*a:b*. Left: Room temperature solutions. Right: Solutions boiled right before the absorption measurement.

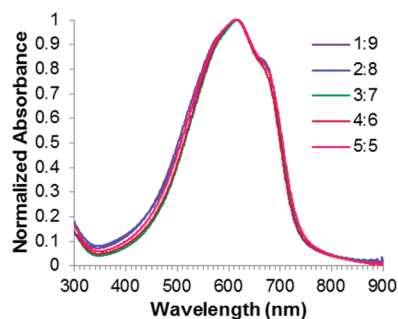


**Figure 5.** UV-vis absorption spectrum of  $C_{12}$ -PTVs-*a:b* thin films spin-coated on cleaned glass slides from hot *o*-dichlorobenzene solutions (90 °C for 1:9, 2:8, and 3:7, 70 °C for 4:6 and 5:5). Concentration: 8 mg/mL DCB for all. Spin rate: 3000 rpm. Spin duration: 30 s. The films were smooth and 40–60 nm thick.

spectra of as-cast  $C_{12}$ -PTVs-*a:b* films (Figure 5) are nearly same, and the vibronic features are clearly seen for all polymers. The absorption cutoff wavelengths of the films are 770 nm, a 74 nm red shift from that of the chloroform solutions (696 nm). Optical bandgaps are estimated to be 1.78 and 1.61 eV in chloroform solution and film, respectively.

**X-ray Diffraction (XRD) Measurements.** Wide angle out-of-plane diffractograms (Figure 6a) were recorded using a Rigaku X-ray diffractometer Model D/max-2200 (Cu K $\alpha$  radiation,  $\lambda = 1.5406$  Å) for  $C_{12}$ -PTV films drop-casted on glass substrate from *o*-dichlorobenzene solutions maintained at different temperatures (90 °C for 0:10 and 1:9, 70 °C for 2:8, 50 °C for 3:7, and RT for 4:6 and 5:5  $C_{12}$ -PTVs). All  $C_{12}$ -PTVs gave the same diffraction peak pattern with strong first-order diffraction peaks and good third-order diffraction peaks. The thickness-normalized peak intensities of  $C_{12}$ -PTV-3:7 are even stronger (by 23%) than those of  $C_{12}$ -PTV-1:9. The peak intensities of  $C_{12}$ -PTV-5:5 are only ~20% weaker than that of  $C_{12}$ -PTV-1:9. It is the first time, to our best knowledge, that crystal packing of  $\pi$ -conjugated polymers is found not strongly affected by its regioregularity. This phenomenon can be attributed mainly to the relatively long separation between side chains, which allows all side chains to be packed in the plane of polymer backbone regardless of regioregularity. All films gave the same  $2\theta$  value (4.85°) of the first diffraction peak (100), corresponding to a  $d$ -spacing of 18.27 Å.

To better understand the thermal behaviors of  $C_{12}$ -PTVs, XRD measurements were performed on selected samples (i.e.,  $C_{12}$ -PTVs-1:9, 3:7 and 5:5) heated at temperatures between

two endothermic peaks (T1) and above the second peaks (T2) (Figure 6b). Heating was conducted in a nitrogen atmosphere, and lasted for one minute to avoid possible oxidation of the polymers especially at T2. The heated samples were immediately quenched by liquid nitrogen to preserve the polymer organization. Heating at T1 enhanced XRD peaks of all polymers tested, while heating at T2 caused all XRD peaks to disappear. The results suggest that the first DSC peaks are due to the transition from crystalline solid to a mesophase, similar to that of RR P3DDT<sup>36</sup> which is characterized by decoupled free “floating” layers,<sup>39</sup> and the second DSC peaks are due to the transition from the mesophase to isotropic liquids. Apparently, higher mobility of polymer at T1 facilitates polymer chains reorganization into a better order, which is reflected in the XRD peak enhancement by heating at T1. X-ray diffraction peak has been used as an evidence for regioregularity of  $C_6$ -PTVs synthesized via the dithiocarbamate precursor route.<sup>40</sup> In the light of this work, more evidence is likely needed to substantiate regioregularity in PTV polymers.

**HOMO/LUMO Energy Levels.** Frontier orbital energies of  $C_{12}$ -PTVs-*a:b* were measured by cyclovoltammetry (Figure 7). The reduction onset potentials of  $C_{12}$ -PTVs-*a:b* films are practically the same (−1.89 eV, referenced to Ag/AgNO<sub>3</sub>) and correspond to a LUMO energy of −2.90 eV, which was calculated from the equation of  $E_{\text{LUMO, polymer}} = (E_{\text{HOMO, Ferro}} - E_{\text{red, polymer}}) + E_{\text{ox, Ferro}}$ , where −4.80 eV was used for  $E_{\text{HOMO, Ferro}}$ , and the oxidation potential energy of ferrocene ( $E_{\text{ox, Ferro}}$ ) was measured to be 0.01 eV. The oxidation onset potentials are in the range of 0.26–0.29 V (with  $C_{12}$ -PTV-0:10 at the higher end and  $C_{12}$ -PTV-5:5 at the lower end) and are averaged at 0.28 V (Table 3). The HOMO energies, calculated from oxidation onset potentials using  $E_{\text{HOMO, polymer}} = (E_{\text{HOMO, Ferro}} - E_{\text{ox, polymer}}) + E_{\text{ox, Ferro}}$ , are also listed in Table 3 and average at −5.07 eV. The average electrochemical energy gap is 2.17 eV. A slight, yet consistent, increase in the HOMO energy is found for  $C_{12}$ -PTVs from 0:10 to 5:5. (See more discussion in the device section)

**Solubility Study.** The initial objective of tuning regioregularity of  $C_{12}$ -PTV was to improve solubility and processability of this class of polymer. Qualitatively, better solubility was observed for less regioregular  $C_{12}$ -PTVs during the polymer synthesis. Semiquantitative solubility tests were performed on all polymer samples. In chloroform,  $C_{12}$ -PTV-0:10 was partially dissolved when the solution was boiled; however, the polymer precipitated out completely, leaving no color in the solution after a few days of storage at room temperature. In sharp contrast,  $C_{12}$ -PTV-5:5 has a solubility of greater than 20 mg/mL in the same solvent at room temperature. In *o*-dichlorobenzene, which was used to dissolve

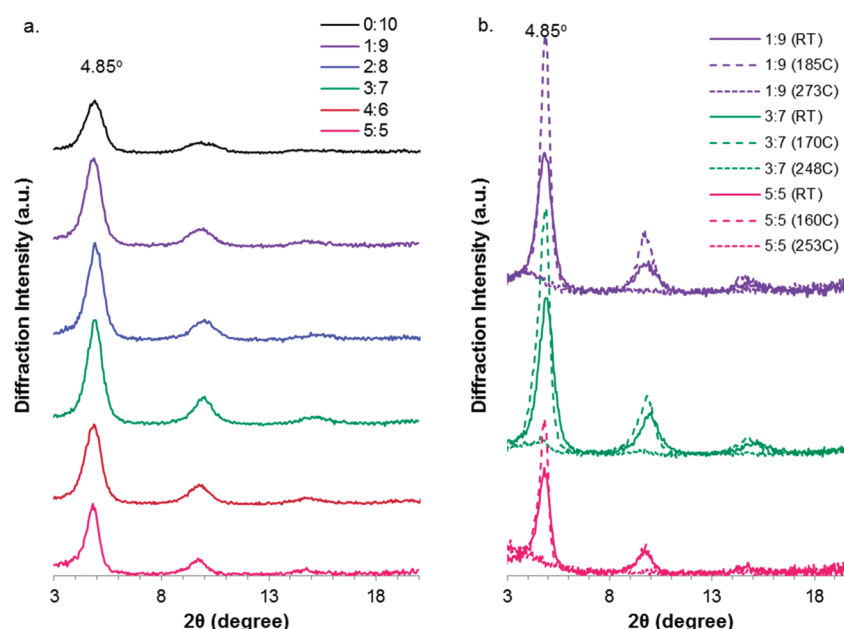


**Figure 6.** Wide angle XRD analysis of C<sub>12</sub>-PTVs-*a:b*. (a) XRD patterns of C<sub>12</sub>-PTV-*a:b* (with thickness normalized). Drop casted films were dried at room temperature. Thicknesses of films are in the range of 4.4–7.0 μm. The background from the glass substrates has been subtracted. (b) XRD measurements of selected samples (i.e., 1:9, 3:7 and 5:5) heated at temperatures between two melting peaks (T<sub>1</sub>) and above the second melting points (T<sub>2</sub>). Correction of an error in ref 32: the XRD peaks of C<sub>12</sub>-PTV-0:10 were a little off due to an error in sample vertical position. The first order peak should be at 2θ = 4.85°, instead of 5.7°.

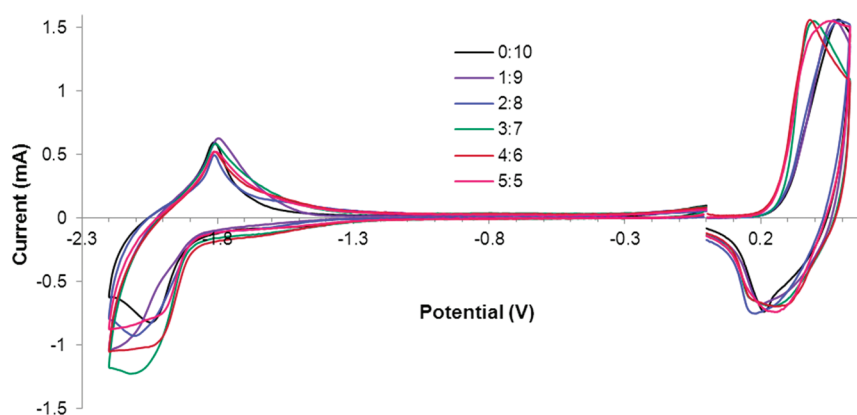


**Figure 7.** Cyclic voltammograms of C<sub>12</sub>-PTVs-*a:b*.

**Table 3.** HOMO Energy of C<sub>12</sub>-PTVs-*a:b* and Performance of C<sub>12</sub>-PTVs-*a:b*/PCBM(1:1) Bulk Heterojunction Solar Cell Devices<sup>a</sup>

| <i>a:b</i> | redn onset (V) | HOMO (eV) | V <sub>oc</sub> (V) | J <sub>sc</sub> (mA/cm <sup>2</sup> ) | FF          | efficiency (%) | no. of cells |
|------------|----------------|-----------|---------------------|---------------------------------------|-------------|----------------|--------------|
| 0:10       | 0.29           | −5.08     | 0.51 (0.51)         | 1.60 (1.48)                           | 0.44 (0.44) | 0.36 (0.33)    | 4            |
| 1:9        | 0.29           | −5.08     | 0.47 (0.46)         | 1.67 (1.55)                           | 0.59 (0.58) | 0.46 (0.41)    | 5            |
| 2:8        | 0.28           | −5.07     | 0.45 (0.44)         | 1.66 (1.60)                           | 0.50 (0.49) | 0.38 (0.34)    | 6            |
| 3:7        | 0.27           | −5.06     | 0.43 (0.43)         | 1.82 (1.61)                           | 0.56 (0.53) | 0.44 (0.37)    | 6            |
| 4:6        | 0.26           | −5.05     | 0.44 (0.43)         | 1.32 (1.18)                           | 0.41 (0.41) | 0.23 (0.21)    | 5            |
| 5:5        | 0.26           | −5.05     | 0.44 (0.43)         | 1.60 (1.42)                           | 0.51 (0.51) | 0.35 (0.31)    | 6            |

<sup>a</sup> Both the best and average (in parentheses) device results are given.

polymers for solar cell device fabrication, all polymers can be dissolved at a concentration of 16 mg/mL at 90–100 °C. During cooling, C<sub>12</sub>-PTV-0:10 started to precipitate at 70–80 °C, 1:9 at

50–70 °C, 2:8 at 40–50 °C, and 3:7 at 30–40 °C. The 4:6 and 5:5 polymers did not precipitate even after the solutions were cooled to the room temperature (25 °C). The higher solubility of

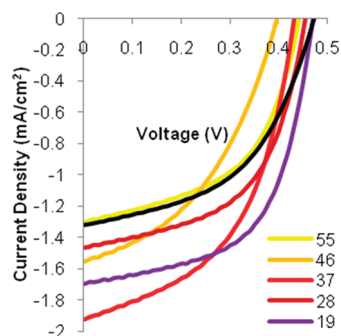


**Figure 8.** Typical  $J$ - $V$  curves of  $C_{12}$ -PTV:PCBM (1:1) solar cell devices.

less regioregular  $C_{12}$ -PTVs may be attributed to the irregularity of side chain domain which is easier for solvent molecules to penetrate.

**Solar Cell Device Fabrication.** It is of great interest to find how the differences in regioregularity, solubility and crystallization tendency affect efficiency of  $C_{12}$ -PTVs-based solar cells. Due to the large number of polymers and variables in film processing and device fabrication, it is beyond the scope of this paper to conduct device optimization for each polymer. A common device structure, i.e., ITO/PEDOT/ $C_{12}$ -PTV:PCBM/Al, and a standard film/device processing procedure was used and is described here. A PEDOT-PSS layer of thickness of 60 nm was first spin coated on ITO glass substrates patterned with eight  $4.5\text{ mm} \times 4.5\text{ mm}$  bottom electrodes.  $C_{12}$ -PTV solutions of the same concentration (15 mg of polymer and 15 mg of PCBM in 1 mL of *o*-dichlorobenzene, fully dissolved at elevated temperatures) were spin-coated at appropriate spin rates (lower for 0:10, higher for 5:5 due to the difference in molecular weight) to give films of the similar thickness (40–50 nm). The films became dry during the spinning period (30 s), and were further dried by vacuuming at room temperature. Thermal annealing was not performed on any sample. Aluminum top electrode was deposited and the devices were tested in a  $N_2$ -filled glovebox.

The  $J$ - $V$  curves of the devices of all polymers are shown in Figure 8. The device performance parameters are summarized in Table 3. The average  $V_{oc}$  decreases from 0.51 V for  $C_{12}$ -PTV-0:10 to 0.43 V for  $C_{12}$ -PTV-5:5. The change in  $V_{oc}$  follows the same trend in HOMO energy,<sup>41</sup> but is slightly larger in magnitude. Although  $V_{oc}$  has been reported to decrease with molecular weight (MW) up to  $8\text{ kg}\cdot\text{mol}^{-1}$  in a fluorene-based oligomers/polymers,<sup>42</sup> a clear effect of MW on  $V_{oc}$  was not observed for RR P3HTs with  $M_n$  in a range of 4500 to  $33400\text{ kg}\cdot\text{mol}^{-1}$ .<sup>43</sup> It is unlikely that polymer molecular weight plays a major role in the trend observed for  $C_{12}$ -PTVs because even the lowest MW polymer ( $C_{12}$ -PTV-0:10) contains 26 repeat units, and no shift in optical absorption was observed from  $C_{12}$ -PTV-0:10 to  $C_{12}$ -PTV-5:5 as was observed for the fluorene-based oligomers/polymers with  $M_n$  up to  $8\text{ kg}\cdot\text{mol}^{-1}$ .<sup>42</sup> It is more likely that the trend in  $V_{oc}$ , as well as HOMO energy, is related to the slight difference in polymer packing in the  $C_{12}$ -PTV films (e.g., distance between stacking  $\pi$ -planes, not detectable with the wide angle XRD technique used in this work). Different  $V_{oc}$  values have been reported for P3HTs of different regioregularity: 0.62, 0.63, and 0.58 V from 86, 90, and 96% RR P3HT, respectively.<sup>44</sup> There appears to be an opposite trend in RR P3HT, which is presumably related to the increase in energy gap with the decrease in

regioregularity.<sup>44</sup> There seems no clear trend in the efficiencies of the preliminary  $C_{12}$ -PTV devices (Table 3), and  $C_{12}$ -PTV-3:7 devices performed practically as well as  $C_{12}$ -PTV-1:9 devices. The slight difference is mainly due to the larger  $V_{oc}$  of  $C_{12}$ -PTV-1:9 devices.  $C_{12}$ -PTV-3:7 devices actually produced significantly higher  $J_{sc}$ . For routine device fabrication,  $C_{12}$ -PTV-3:7 is a better choice than the highly regioregular ones which can precipitate out of solutions during the solution transferring process and, therefore, requires more practice to obtain good films. The best efficiencies of the preliminary devices obtained from  $C_{12}$ -PTV-1:9 and -3:7 are twice as high as the best value reported for  $C_{12}$ -PTV prepared by the Stille coupling method.<sup>15</sup>

## 4. CONCLUSIONS

A series of  $C_{12}$ -PTVs with different regioregularity have been synthesized and characterized. The aromatic and olefinic proton NMR peaks of this class of polymers are clearly assigned. This series of polymers allow us to conduct a systematic study of the effect of regioregularity on the processability, crystallinity, and optoelectronics properties of  $C_{12}$ -PTVs. For the first time, it is found that good crystallinity can exist in regiorandom  $C_{12}$ -PTVs. This finding suggests that the appearance of XRD peaks may not be used as an evidence for any degree of regioregularity in  $C_n$ -PTV structures. For  $C_{12}$ -PTVs and, possibly, related polymers, low regioregularity samples are likely better choices for solar cell device fabrication due to their much better processability and comparable crystallinity and device efficiency. It is also found that all  $C_{12}$ -PTVs-*a:b* have the same optical energy gap, but, more regioregular ones have lower HOMO energies and give higher  $V_{oc}$ s in solar cells. A more detailed study of the series of polymers in thin films and devices is currently underway with emphasis on 1:9, 3:7, and 5:5 polymers. Measurement of charge mobility in and across the polymer films will also be performed through collaborations.

## ■ ASSOCIATED CONTENT

**Supporting Information.**  $^1\text{H}$  and  $^{13}\text{C}$  NMR spectra of compounds **1**, **4**–**7**, three model compounds (H–T, H–H, and T–T), and polymers. This material is available free of charge via the Internet at <http://pubs.acs.org>.

## ■ AUTHOR INFORMATION

### Corresponding Author

\*E-mail: (C.Z.) [cheng.zhang@sdstate.edu](mailto:cheng.zhang@sdstate.edu); (S.-S.S.) [ssun@nsu.edu](mailto:ssun@nsu.edu).

## ■ ACKNOWLEDGMENT

This work is supported by the Department of Defense through award W911NF-06-1-0488 and the National Science Foundation through award HRD-0931373. Lafalce and Jiang are grateful to the support from New Energy Technologies, Inc. and Florida High Tech Corridor Matching Fund.

## ■ REFERENCES

- (1) Liang, Y.; Yu, L. *Polym. Rev.* **2010**, *50*, 454.
- (2) Cheng, Y.-J.; Yang, S.-H.; Hsu, C.-S. *Chem. Rev.* **2009**, *109*, 5868.
- (3) Facchetti, A. *Chem. Mater.* **2011**, *23*, 733.
- (4) Thompson, B. C.; Frechet, J. M. J. *Angew. Chem., Inter. Ed.* **2008**, *47*, 58.
- (5) Osaka, I.; McCullough, R. D. *Acc. Chem. Res.* **2008**, *41*, 1202.



- (6) Chen, T.-A.; Wu, X.; Rieke, R. D. *J. Am. Chem. Soc.* **1995**, *117*, 233.
- (7) Bao, Z.; Dodabalapur, A.; Lovinger, A. J. *Appl. Phys. Lett.* **1996**, *69*, 4108.
- (8) Brown, P. J.; Friend, R. H.; Nielsen, M. M.; Bechgaard, K.; Langeveld-Voss, B. M. W.; Spiering, A. J. H.; Janssen, R. A. J.; Meijer, E. W.; Herwig, P.; de Leeuw, D. M. *Nature* **1999**, *401*, 685.
- (9) Li, G.; Shrotriya, V.; Huang, J.; Yao, Y.; Moriarty, T.; Emery, K.; Yang, Y. *Nat. Mater.* **2005**, *4*, 864.
- (10) Kim, Y.; Choulis, S. A.; Nelson, J.; Bradley, D. D. C.; Cook, S.; Durrant, J. R. *Appl. Phys. Lett.* **2005**, *86*, 063502.
- (11) Nguyen, L. H.; Hoppe, H.; Erb, T.; Günes, S.; Gobsch, G.; Sariciftci, N. S. *Adv. Funct. Mater.* **2007**, *17*, 107.
- (12) Lee, J. K.; Ma, W. L.; Brabec, C. J.; Yuen, J.; Moon, J. S.; Kim, J. Y.; Lee, K.; Bazan, G. C.; Heeger, A. J. *J. Am. Chem. Soc.* **2008**, *130*, 3619.
- (13) Tajima, K.; Suzuki, Y.; Hashimoto, K. *J. Phys. Chem. C* **2008**, *112*, 8507.
- (14) Henckens, A.; Knipper, M.; Polec, I.; Manca, J.; Lutsen, L.; Vanderzande, D. Belg. *Thin Solid Films* **2004**, *451–452*, 572.
- (15) Smith, A. P.; Smith, R. R.; Taylor, B. E.; Durstock, M. F. *Chem. Mater.* **2004**, *16*, 4687.
- (16) Van De Wetering, K.; Brochon, C.; Ngov, C.; Hadziioannou, G. *Macromolecules* **2006**, *39*, 4289.
- (17) Banishoeib, F.; Henckens, A.; Fourier, S.; Vanhooyland, G.; Breselge, M.; Manca, J.; Cleij, T. J.; Lutsen, L.; Vanderzande, D.; Nguyen, L. H.; Neugebauer, H. *Thin Solid Films* **2008**, *516*, 3978.
- (18) Nguyen, L. H.; Guenes, S.; Neugebauer, H.; Sariciftci, N. S.; Banishoeib, F.; Henckens, A.; Cleij, T.; Lutsen, L.; Vanderzande, D. *Sol. Energy Mater. Sol. Cells* **2006**, *90* (17), 2815.
- (19) Hou, J.; Tan, Z.; He, Y.; Yang, C.; Li, Y. *Macromolecules* **2006**, *39*, 4657.
- (20) Horie, M.; Shen, I.-W.; Tuladhar, S. M.; Leventis, H.; Haque, S. A.; Nelson, J.; Saunders, B. R.; Turner, M. L. *Polymer* **2010**, *51*, 1541.
- (21) Kim, J. Y.; Yang, Q.; Stevens, D. M.; Ugurlu, O.; Kalihari, V.; Hillmyer, M. A.; Frisbie, C. D. *J. Phys. Chem. C* **2009**, *113*, 10790.
- (22) Qin, Y.; Hillmyer, M. A. *Macromolecules* **2009**, *42*, 6429.
- (23) Blohm, M. L.; Pickett, J. E.; Van Dort, P. C. *Macromolecules* **1993**, *26*, 2704.
- (24) Van De Wetering, K.; Brochon, C.; Ngov, C.; Hadziioannou, G. *Macromolecules* **2006**, *39*, 4289.
- (25) Loewe, R. S.; McCullough, R. D. *Chem. Mater.* **2000**, *12*, 3214.
- (26) Huitema, H. E. A.; Gelinck, G. H.; van der Putten, J. B. P. H.; Kuijk, K. E.; Hart, C. M.; Cantatore, E.; Herwig, P. T.; van Breemen, A. J. J. M.; de Leeuw, D. M. *Nature* **2001**, *414*, 599.
- (27) Fuchigami, H.; Tsumura, T.; Koezuka, H. *Appl. Phys. Lett.* **1993**, *63*, 1372.
- (28) Yamada, S.; Tokito, S.; Tsutsui, T.; Saito, S. *J. Chem. Soc., Chem. Commun.* **1987**, 1448.
- (29) Nguyen, L. H.; Günes, S.; Neugebauer, H.; Sariciftci, N. S.; Banishoeib, F.; Henckens, A.; Cleij, T.; Lutsen, L.; Vanderzande, D. *Sol. Energy Mater. Sol. Cells* **2006**, *90*, 2815.
- (30) Giroto, C.; Cheyns, D.; Aernouts, T.; Banishoeib, F.; Lutsen, L.; Cleij, T. J.; Vanderzande, D.; Genoe, J.; Poortmans, J.; Heremans, P. *Org. Electron.* **2008**, *9*, 740.
- (31) Huo, L.; Chen, T. L.; Zhou, Y.; Hou, J.; Chen, H.-Y.; Yang, Y.; Li, Y. *Macromolecules* **2009**, *42*, 4377.
- (32) Zhang, C.; Matos, T.; Li, R.; Sun, S.-S.; Lewis, J. E.; Zhang, J.; Jiang, X. *Polym. Chem.* **2010**, *1*, 663.
- (33) Suzuki, Y.; Hashimoto, K.; Tajima, K. *Macromolecules* **2007**, *40*, 6521.
- (34) Mozer, A. J.; Denk, P.; Scharber, M. C.; Neugebauer, H.; Sariciftci, N. S.; Wagner, P.; Lutsen, L.; Vanderzande, D. *J. Phys. Chem. B* **2004**, *108* (17), 5235.
- (35) Pankay, S.; Hempel, E.; Beiner, M. *Macromolecules* **2009**, *42*, 716.
- (36) Causin, V.; Marega, C.; Marigo, A.; Valentini, L.; Kenny, J. M. *Macromolecules* **2005**, *38*, 409.
- (37) McCullough, R. D.; Lowe, R. D.; Jayaraman, M.; Anderson, D. L. *J. Org. Chem.* **1993**, *58*, 904.
- (38) Oliveira, F. A. C.; Cury, L. A.; Righi, A.; Moreira, R. L.; Guimarães, P. S. S.; Matinaga, F. M.; Pimenta, M. A.; Nogueira, R. A. *J. Chem. Phys.* **2003**, *119*, 9777.
- (39) Prosa, T. J.; Winokur, M. J.; Moulton, J.; Smith, P.; Heeger, A. J. *Macromolecules* **1992**, *25*, 4364.
- (40) Banishoeib, F.; Adriaenssens, P.; Berson, S.; Guillerez, S.; Douheret, O.; Manca, J.; Fourier, S.; Cleij, T. J.; Lutsen, L.; Vanderzande, D. *Sol. Energy Mater. Sol. Cells* **2007**, *91*, 1026.
- (41) Ishwara, T.; Bradley, D. D. C.; Nelson, J.; Ravirajan, P.; Vanseveren, I.; Cleij, T.; Vanderzande, D.; Lutsen, L.; Tierney, S.; Heeney, M.; McCulloch, I. *Appl. Phys. Lett.* **2008**, *92*, 053308.
- (42) Müller, C.; Wang, E.; Andersson, L. M.; Tvingstedt, K.; Zhou, Y.; Andersson, M. R.; Inganäs, O. *Adv. Funct. Mater.* **2010**, *20*, 2124.
- (43) Hiorns, R. C.; de Bettignies, R.; Leroy, J.; Bailly, S.; Firon, M.; Sentein, C.; Khoukh, A.; Preud'homme, H.; Dagon-Lartigau, C. *Adv. Funct. Mater.* **2006**, *16*, 2263.
- (44) Woo, C. H.; Thompson, B. C.; Kim, B. J.; Toney, M. F.; Frechet, J. M. J. *J. Am. Chem. Soc.* **2008**, *130*, 16324.